Hydrogen-Transferred Radical Cations of NADH Model Compounds. 3. 1,8-Acridinediones

Andrzej Marcinek, Jan Adamus, and Jerzy Gębicki*

Institute of Applied Radiation Chemistry, Technical University, 90-924 Lodz, Poland

Matthew S. Platz

Newman and Wolfrom Laboratory of Chemistry, The Ohio State University, Columbus, Ohio 43210

Paweł Bednarek†

Institute of Physical Chemistry, University of Fribourg, Perolles, CH-1700 Fribourg, Switzerland

Received: October 27, 1999

Two different tautomeric forms of radical cations generated from 1,8-acridinediones were characterized by steady-state methods, pulse radiolysis, and laser flash photolysis techniques. In solution the primarily formed keto radical cations tautomerize in less than 1 ns to the corresponding enol radical cations. This process is significantly retarded in cryogenic glasses.

1. Introduction

In the refs 1−3 we discussed processes leading to the formation of enol radical cations of NADH analogues. It was shown that such species can be formed by both intra- and intermolecular processes. 1,8-Acridinediones can also be considered as NADH analogues where both oxygen atoms are locked in a geometry suitable for intramolecular hydrogen atom transfer in the corresponding radical cations. Moreover, the hydrogen atoms attached to the carbon atom in the 9-position are sterically protected from intermolecular reactions by the two carbonyl groups.[4] In the present study we used the two compounds 3,3,6,6,10-pentamethyl-3,4,6,7,9,10-hexahydro-1,8-(2*H*,5*H*)-acridinedione (**1HK**) and its oxidized form $\mathbf{1}^+$.

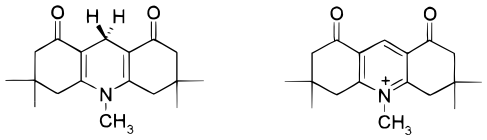

1HK **1⁺**

In a series of papers Mohan et al.[5−8] described the redox properties of this group of compounds and spectroscopically characterized the radical cations, anions, and radicals formed in these processes. Acid−base equilibria were also determined. However, these authors did not consider the possibility of radical cation tautomerization.

Our preceding studies on NADH analogues led us to address the question of radical cation tautomerization in 1,8-acridinediones. The transient species generated from **1HK** and its oxidized form $\mathbf{1}^+$ by steady-state and pulse radiolysis as well as by laser flash photolysis techniques are characterized both spectroscopically and kinetically, and assignments of these transient species are proposed.

2. Results and Discussion

In the studies of the redox properties of 1,8-acridinediones Mohan et al.[5] characterized two transient species: the radical cation absorbing at 305 and 560 nm and the radical absorbing at 650 nm. Both species participate in acid−base equilibrium. It was concluded that the observed pH dependence is due to the deprotonation of the acridinedione radical cation. However, according to our studies of NADH model compounds, two different tautomeric forms of radical cations should be considered.[1−3] Moreover, the radical cation formed on protonation of the radical is usually different from the primary radical cation obtained upon ionization.

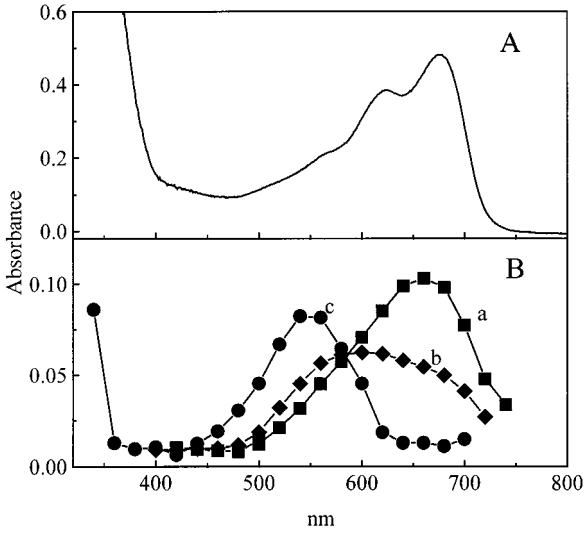

Figure 1. Transient absorption spectra observed upon radiolysis. (A) $\mathbf{1}^+$ (4×10^{-2} M) in 2-propanol matrix (77 K): dose, 10 kGy; thickness of the sample, 3 mm. (B) $\mathbf{1}^+$ (4×10^{-3} M) in aqueous solution (N_2O, 2-propanol [1 M]): dose, 50 Gy; thickness of the sample, 1 cm; $T =$ 25 °C; spectra collected 9×10^{-7} s after a 17 ns pulse at pH 6 (a), pH 5 (b), and pH 3 (c).

The absorption spectrum obtained upon radiolysis of $\mathbf{1}^+$ embedded in an 2-propanol matrix is presented in Figure 1A. The electrons generated in alcoholic glasses are effectively captured by the cations $\mathbf{1}^+$, leading to formation of radicals $\mathbf{1}^{\bullet}$. When the concentration of the $\mathbf{1}^+$ salt was reduced, the observed

† On leave from the Institute of Applied Radiation Chemistry, Technical University, 90-924 Lodz, Poland.

10.1021/jp993817r CCC: $19.00
Published on Web 01/07/2000

absorption spectrum showed a mixture of the radical and solvated electron absorptions. As expected, photobleaching of the solvated electrons led to a concomitant increase in the radical absorption. This confirms that upon reaction of the photolabile electrons with cations $\mathbf{1}^+$, radicals $\mathbf{1}^\bullet$ are formed.

The transient absorption band at 670 nm arises also when electrons are generated by radiolysis of aqueous solutions of $\mathbf{1}^+$ at neutral pH. The same product is formed when acetone ketyl radical is acting as a reducing agent in aqueous solutions containing 2-propanol (see Figure 1B, curve a). An assignment of this absorption band to the radical $\mathbf{1}^\bullet$ remains in agreement with the findings and conclusions of Mohan et al.[5]

In acidic solution (pH 3, curve c in Figure 1B) the product of radiolysis is characterized by an absorption at around 550 nm. Since the reduction mechanism remains unchanged, i.e., cations are reduced by electrons (unless these are completely captured by protons) and acetone ketyl radicals in the primary process, this absorption can be assigned to the radical cation formed on protonation of the radical:

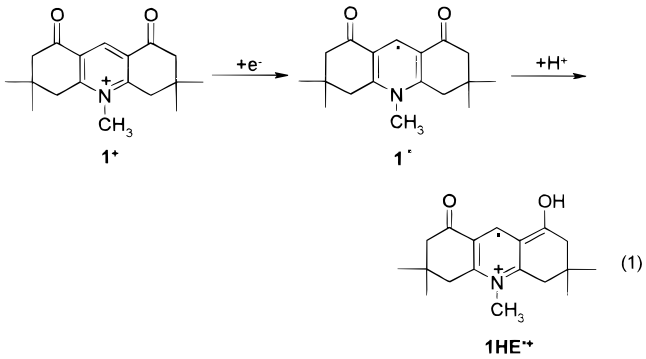

(1)

In view of the results from our previous studies, protonation occurs probably at one of the carbonyl groups; i.e., the radical cation arises in the enol form $\mathbf{1HE}^{\bullet+}$. At intermediate pH (curve b in Figure 1B) both species are observed in the transient spectrum, indicating an acid−base equilibrium between these forms. The estimated value of pK_a is about 5, which is in the range of pK_a values found for NADH models described in the preceding paper in this series.[3]

As in previous cases,[2,3] a clear difference should be observed between the radical cations generated upon protonation of $\mathbf{1}^\bullet$ and upon direct ionization of the reduced compound **1HK**.

The spectrum detected after radiolysis of **1HK** embedded in a 2-chlorobutane (or Freon mixture) matrix shows surprising similarity to the radical spectrum characterized in an alcoholic matrix (the spectra are compared in Figure 2). However, under these experimental conditions formation of the radical cation $\mathbf{1HK}^{\bullet+}$ rather than the radical $\mathbf{1}^\bullet$ is expected:

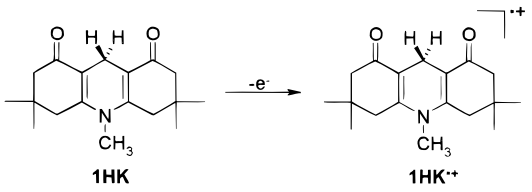

(2)

The formation of $\mathbf{1}^\bullet$ by deprotonation of $\mathbf{1HK}^{\bullet+}$ should be observed only upon matrix softening, which enables diffusion and allows intermolecular processes to proceed.[9,10]

Moreover, in pulse radiolysis experiments, spectrum a in Figure 2 was observed immediately after the electron pulse even at 30 K. Under such conditions intermolecular processes can be excluded. A similar spectrum was also observed upon ionization of **1HK** in an argon matrix.[11] Hence, the 680 nm band in Figure 2 (curve a) can only be assigned to the primary radical cation $\mathbf{1HK}^{\bullet+}$.[12]

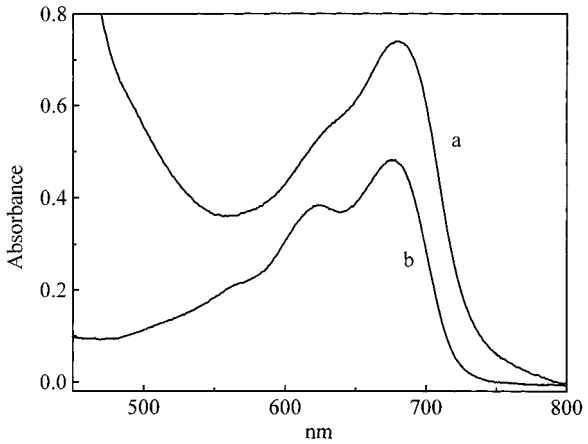

Figure 2. (a) Spectrum observed upon ionization of **1HK** (saturated solution) embedded in 2-chlorobutane matrix at 30 K: radiation dose, 20 kGy; thickness of the sample, 3 mm. (b) Spectrum, originally shown in Figure 1A, given for comparison.

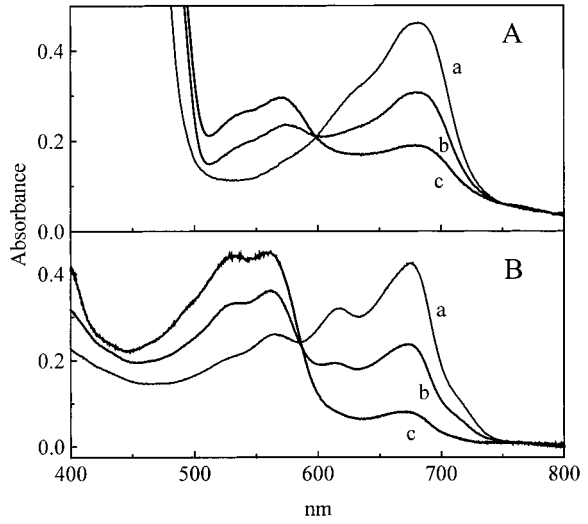

Figure 3. Changes introduced by thermal relaxation (annealing) of the irradiated matrix: (A) 2-chlorobutane matrix containing **1HK** (see Figure 2, curve a) annealed at 100 K for 5 min (a), 20 min (b), and 40 min (c); (B) Isopropanol matrix containing $\mathbf{1}^+$ (see Figure 1A) annealed at 120 K for 10 min (a), at 125 K for 10 min (b), and at 125 K for 20 min (c).

A clear difference exists between the primary product of direct ionization of **1HK** (Figure 2, spectrum a) and the product of electron−proton addition to $\mathbf{1}^+$ (Figure 1B, curve c), which suggests the occurrence of two different (tautomeric) forms of the radical cation.

Thermal relaxation of the 2-chlorobutane matrix containing **1HK** and the radical cation leads to observation of effects analogous to those previously observed with NADH analogues.[3] Initially, some small shifting and narrowing of the absorption band is observed, which is followed by its slow decay at higher temperatures. The decay is accompanied by a simultaneous growth of an absorption band at around 550 nm (Figure 3A). Since this product is formed in a secondary process, it can be rationally assigned either to the radical or to the enol radical cation obtained on protonation of $\mathbf{1}^\bullet$ (see above). Since only the latter species possesses an absorption in this spectral region (Figure 1B, trace c), the observed process can be viewed as a tautomerization.

In some cases both radical cations can be observed simultaneously because of both intra- or intermolecular tautomerization processes. According to B3LYP/6-31G* calculations,[13] 1,8-acridinedione also shows an inversion of the relative stabilities of the keto and enol tautomers on ionization, similar to that found in the other NADH model compounds studied to date.[1−3] Enolization is endothermic by around 41.2 kcal/mol in **1HK** but exothermic by about 10.6 kcal/mol in **1HK**$^{\bullet+}$; i.e., enolization of the radical cation is thermochemically feasible. However, since the transformation of the two species represented by the absorptions at 680 and 550 nm, respectively, is observed only upon thermal relaxation (softening) of the matrix, the formation of the 550 nm species must be due to an intermolecular process.

Thermal relaxation of a 2-propanol matrix containing **1**$^+$ irradiated at 77 K (see Figure 3B) also leads to the decay of the radical absorption band at 670 nm and to parallel formation of a product absorbing at 550 nm. By analogy to the results obtained from radiolysis of aqueous or alcoholic liquid solutions, we assign this product to the enol radical cation formed by protonation of the radical. If the radical is sufficiently basic, the protonation process can take place in alcoholic matrices.[3]

Since diffusion is allowed under these conditions, other intermolecular reactions can compete with protonation. The first one is dimerization of the radicals.[3,14−16] Indeed this process is observed on a longer time scale in aqueous solution ($2k/(\epsilon l) = 3 \times 10^4$ s^{-1}). However, the dimer absorbs at about 390 nm, which allows us to exclude this product as a candidate for an alternative assignment of the 550 nm absorption band.

Sridivya et al.[17] have shown by means of electrochemical methods that the 1,8-acridinedione radical can detach a hydrogen atom from the carbon at the 4-position (side ring). This product possesses absorption bands located at 356 nm with a broad weak shoulder around 520 nm. On the basis of these spectral features, this species can also be excluded as a possible product formed upon thermal relaxation of the matrices.

Comparing the spectra of the transient species obtained from **1HK** to those of the related *bicyclic* compound 1-methyl-1,4,7,8-tetrahydro-5(6*H*)-quinolinone[2,3] (**2HK**)[18] reveals that the introduction of the second carbonyl group leads to substantial but distinctly variable red shifts in the different spectra (see Table 1). To understand these shifts and in particular their variation between the different kinds of transients, we carried out electronic structure calculations by the recently introduced time-dependent density functional response theory (TD-DFRT).

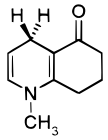

2HK

These calculations showed that the observed absorption bands are described predominantly (80%−90%) by a single excitation to the *first* π excited state in the case of the keto radical cations ($\pi_4 \rightarrow \pi_5$ excitation) and to the *second* π excited state in the neutral radicals ($\pi_6 \rightarrow \pi_8$*) and the enol radical cations ($\pi_6 \rightarrow \pi_8$*), both of which have also several very weak $n_O \rightarrow \pi$ transition that will not be considered here. Therefore, a consideration of the involved MOs and their energies (see Figure 4) should permit a simple rationalization of the shifts. In the case of the keto radical cations the MOs π_4 and π_5 have comparable coefficients at positions 2 and 3 of the 1,4-dihydropyridine ring, respectively; hence, their energy changes only a little on attachment of the second cyclohexanone ring.

TABLE 1: Comparison of the Experimentally Observed Absorption Bands of Transient Species Generated from 1HK and 2HK to the Electronic Transitions Predicted by the TD-B3LYP/6-31G* Method

	experimental			TD-B3LYP/6-31G*		
	2HK	**1HK**	shift	**2HK** (*f*)[a]	**1HK** (*f*)[a]	shift
keto radical cations	610 nm	680 nm	70 nm (0.21 eV)	520 nm[b] (0.045)	590 nm[c] (0.057)	70 nm (0.28 eV)
enol radical cations	455 nm	550 nm	95 nm (0.47 eV)	380 nm[d,e] (0.056)	485 nm[d] (0.075)	105 nm (0.71 eV)
radicals	490 nm	670 nm	180 nm (0.68 eV)	400 nm[d,f] (0.061)	630 nm[d,f] (0.017)	230 nm (1.13 eV)

[a] Oscillator strength for calculated electronic transition. [b] Second excited state above a weak $n_O \rightarrow \pi$ transition in the near-IR. [c] Third excited state above two weak $n_O \rightarrow \pi$ transitions in the near-IR. [d] Second excited state above the HOMO → LUMO ($\pi \rightarrow \pi$*) excitation in the near-IR. [e] For a complete discussion of the electronic structure of the enol radical cation, **2HE**$^{\bullet+}$, see ref 2. [f] In the radicals, the $n_O \rightarrow \pi$ lie above the $\pi \rightarrow \pi$* transitions.

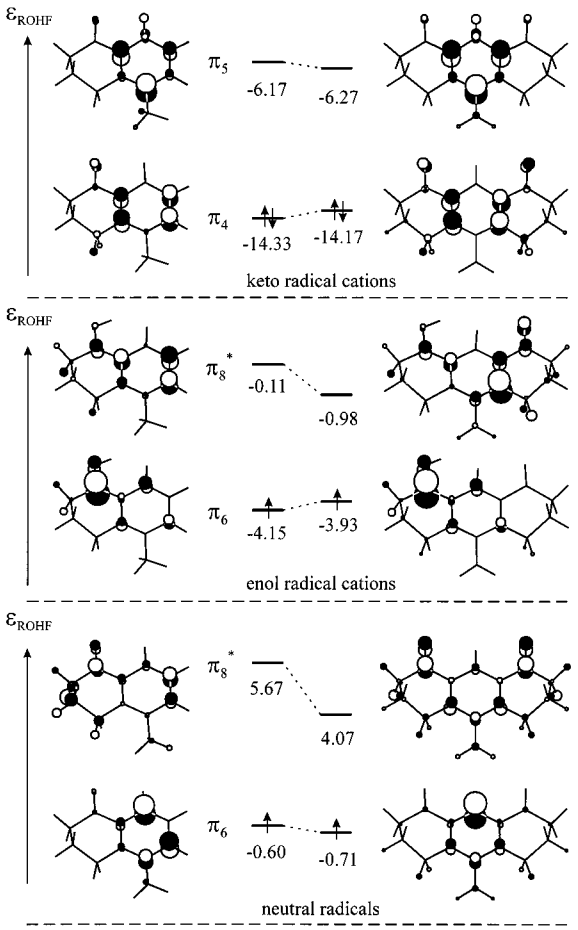

Figure 4. MOs involved in the electronic transitions listed in Table 1. Wave functions and orbital energies from ROHF/3-21G calculations at B3LYP/6-31G* optimized geometries. Area of AO spheres is proportional to coefficients.

Their energy difference shrinks by 0.26 eV, a number that is commensurate with the 0.21 eV red shift of the absorption on going from **2HK**$^{\bullet+}$ to **1HK**$^{\bullet+}$.

In the enol radical cations the coefficients of the MOs π_6 (HOMO) and π_8* in positions 2 and 3, respectively, are more dissimilar. Thus, π_6 is raised by only 0.22 eV, whereas π_8* is lowered by 0.87 eV, which leads to a reduction in the energy gap between these two MOs of 1.09 eV. Indeed, the red shift observed on going from **2HE**$^{\bullet+}$ to **1HE**$^{\bullet+}$ is more than twice as

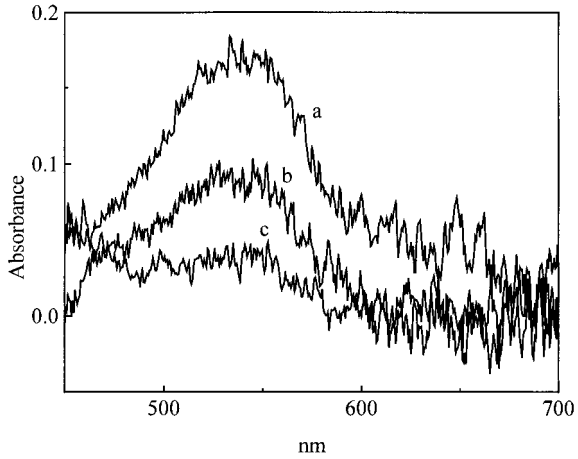

Figure 5. Transient absorption spectra observed by laser flash photolysis (351 nm) of **1HK** in acetonitrile solution containing $CHBr_3$ as an electron scavenger collected at different times after the laser pulse: 100 ns (a), 4 μs (b), and 20 μs (c).

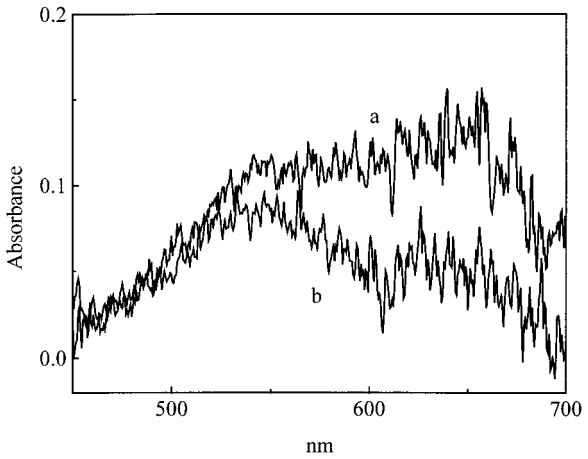

Figure 6. Transient absorption spectra observed by laser flash photolysis (351 nm) of **1HK** in acetonitrile solution containing $\mathbf{1}^+$ as an electron scavenger collected at 1.7 μs (a) and 10 μs (b) after the laser pulse.

large (in electronvolts) as that for $\mathbf{2HK}^{\bullet+}$ to $\mathbf{1HK}^{\bullet+}$, in agreement with the above semiquantitative prediction. Finally, in the radicals, the π_6 HOMO has a near-zero coefficient at C-3, whereas π_8* has a large one. Hence, it is not surprising that the π_6 energy changes by only 0.11 eV but π_8* is stabilized by 1.6 eV on attachment of the second cyclohexanone ring (note that the shape of the MO π_8* changes much more than that of any of the other MOs depicted in Figure 4). This results in a 1.5 eV narrowing of the $\pi_6-\pi_8$* energy gap, which expresses itself in the unusually large red shift of the corresponding absorption band.

Although the shifts are overestimated by TD-B3LYP, the trends are rather well reproduced. Thus, the above MO analysis allows us to understand, for example, why the spectra of $\mathbf{1HK}^{\bullet+}$ and $\mathbf{1}^{\bullet}$ are nearly superimposable (Figure 2), whereas the corresponding absorption bands of the closely related species $\mathbf{2HK}^{\bullet+}$ and $\mathbf{2}^{\bullet}$ are separated by 120 nm.

Slow formation of the 550 nm absorption band under matrix conditions is in contrast with the observation of a fast rise of this absorption in the pulse radiolysis of solution by Mohan et al.[5] We therefore decided to probe this process using flash photolysis in acetonitrile for radical cation generation.

In the absence of electron scavengers, the triplet absorption at around 620 nm dominates in the transient spectrum in accordance with earlier observations.[19,20] However, in the presence of electron scavengers a new product with absorption at 550 nm and a lifetime over 10 μs is observed next to the triplet. Use of the strong electron acceptor $CHBr_3$ enhances the effectiveness and rate of electron transfer such that only the absorption at 550 nm is clearly seen in the spectrum immediately after the laser pulse (within a resolution of the laser flash photolysis system, i.e., less than 1 ns) (Figure 5). This absorption can be assigned to the enol radical cation. No other intermediates can be observed even on lowering the temperature to -25 °C. This means that the rate of enol radical cation formation is comparable to the rate of an electron detachment from the triplet state of the excited dione.

It is also worth mentioning that $\mathbf{1}^+$ can act as an effective electron scavenger. Initially, the triplet absorption dominates the transient spectra. However, on longer time scales a mixture of two products can be distinguished: the enol radical cation with absorption at 550 nm and the radical formed on reduction of the $\mathbf{1}^+$ with absorption at 650 nm (curves a and b in Figure 6).

SCHEME 1

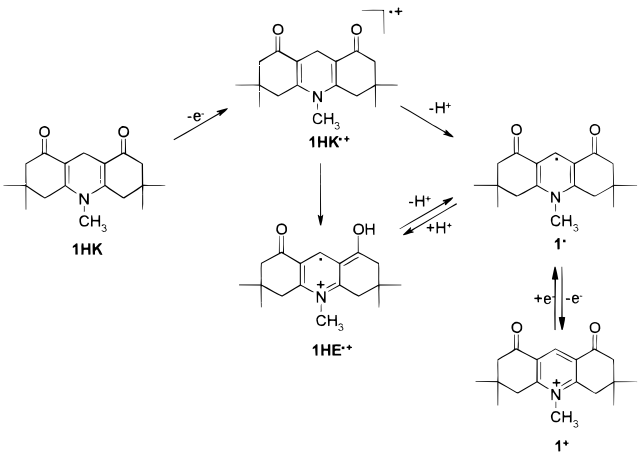

Both these experiments and especially the extremely fast appearance of the enol radical cation indicate that intramolecular hydrogen atom transfer is responsible for its formation upon ionization of 1,8-acridinediones in solution.

3. Conclusions

The results presented here strongly support an assignment of the 550 nm absorption band to the enol radical cation of **1HK**. The tautomerization process can take place either intramolecularly or with assistance of a neutral substrate or solvent molecules via intermolecular processes. In solution the tautomerization process was very fast. Scheme 1 summarizes the processes observed.

4. Experimental Section

Compounds. *3,3,6,6,10-Pentamethyl-3,4,6,7,9,10-hexahydro-1,8(2H,5H)-acridinedione (**1HK**)*. **1HK** was prepared according to the published procedure.[17]

3,3,6,6,10-Pentamethyl-3,4,6,7-tetrahydro-[1,8(2H,5H)-dione]-acridinium Chloride ($\mathbf{1}^+$). **1HK** (0.29 g, 1 mmol) was electrolyzed in acetonitrile containing 0.1 M TBAP at a potential of 1.1 V vs 0.01 M Ag/Ag^+. After completion of the electrolysis the solvent was evaporated in vacuo and the residue was treated with concentrated KOH. The red product was extracted with ethyl ether and the extract concentrated to give red crystals that were dissolved in methanol. The solution was acidified with

diluted hydrochloric acid and concentrated to dryness to give a light-yellow solid that was crystallized from methanol−ether, mp 202 °C dec.

Radiolysis. A description of our pulse radiolysis system based on a linear accelerator, and the procedures for steady-state and time-resolved radiolytic measurements are given elsewhere.[21,22]

Photolysis. The laser photolysis system employed a Lumonics TE-861-4 excimer laser (351 nm, 60 mJ, 17 ns) or a Nd:YAG laser (Continium PY62C-10, 355 nm, 30 mJ, 150 ps). The absorbance of the samples was close to 1.0 at the wavelength of the laser. Solutions were kept in quartz cuvettes and deoxygenated prior to photolysis by purging with argon. An EG&G Princeton Applied Research model 1460 optical multichannel analyzer (OMA) was used to record transient absorption spectra. The laser apparatus is described in more detail elsewhere.[23]

Quantum Chemical Calculations. The geometries of all species were optimized by the B3LYP density functional method[24,25] as implemented in the Gaussian 94 program,[26,27] using the 6-31G* basis set. Relative energies were calculated at the same level. Excited-state calculations on the transient species were carried out by the TD-DFRT procedure[28] as implemented in the Gaussian 98 program (keyword TD),[29] using again the B3LYP functional and the 6-31G* basis set. The MOs in Figure 4 were plotted with the MOPLOT program,[30] which gives a schematic representation of the MOs' nodal structures in a ZDO-type approximation.[31]

Acknowledgment. We thank Professor Thomas Bally for discussion and comments. This work was supported by the U.S.−Poland M. Skłodowska−Curie Joint Fund (Grant No. MEN/NSF-97-303) and the Swiss National Science Foundation (Grant No. 2000-053568.00). J.G. thanks the Foundation on behalf of Polish Science for support from the program "Subsidies for Scholars".

Supporting Information Available: Listing of total energies and Cartesian coordinates from the B3LYP calculations for the compounds in Table 1 in ASCII format available through the Internet. This material is available free of charge via the Internet at http://pubs.acs.org.

References and Notes

(1) Gębicki, J.; Marcinek, A.; Adamus, J.; Paneth, P.; Rogowski, J. *J. Am. Chem. Soc.* **1996**, *118*, 691.

(2) Marcinek, A.; Adamus, J.; Huben, K.; Gębicki, J.; Bartczak, T. J.; Bednarek, P.; Bally, T. *J. Am. Chem. Soc.*, in press.

(3) Marcinek, A.; Rogowski, J.; Adamus, J.; Gębicki, J.; Bednarek, P.; Bally. T. *J. Phys. Chem. A* **2000**, *104*, 718.

(4) Singh, S.; Chhina, S.; Sharma, V. K. *J. Chem. Soc., Chem. Commun.* **1982**, 453.

(5) Mohan, H.; Srividya, N.; Ramamurthy, P.; Mittal, J. P. *J. Chem. Soc., Faraday Trans.* **1996**, *92*, 2353.

(6) Mohan, H.; Mittal, J. P.; Venkatachalapathy, B.; Srividya, N.; Ramamurthy, P. *J. Chem. Soc., Faraday Trans.* **1997**, *93*, 4269.

(7) Mohan, H.; Srividya, N.; Ramamurthy, P.; Mittal, J. P. *J. Phys. Chem. A* **1997**, *101*, 2931.

(8) Mohan, H.; Mittal, J. P.; Srividya, N.; Ramamurthy, P. *J. Phys. Chem. A* **1998**, *102*, 4444.

(9) Shida, T. *Electronic absorption spectra of radical ions*; Elsevier: Amsterdam, 1988.

(10) Marcinek, A.; Rogowski, J.; Adamus, J.; Gębicki, J.; Platz, M. S. *J. Phys. Chem.* **1996**, *100*, 13539.

(11) Bednarek, P.; Gębicki, J.; Bally, T. Unpublished results.

(12) Assignment of the 680 nm absorption band to the primary radical cation could be incorrect only if one assumes its fast intramolecular transformation. Also a high degree of aggregation of neutral compound prior to ionization could facilitate proton transfer within ionized aggregates and radical formation. An assignment of this band to the radical would imply instability of the initially formed radical cation, in contrast to the observed stability of the species absorbing at 550 nm. Moreover, it would also support an assignment of the latter species to the more stable enol radical cation.

(13) For reasons of computational economy all calculations presented in this study and related to **1HK** were limited to the 10-methyl-3,4,6,7,9,10-hexahydro-1,8(2*H*,5*H*)-acridinedione (i.e., without four methyl groups attached to 3 and 6 positions of side rings).

(14) Land, E. J.; Swallow, A. J. *Biochim. Biophys. Acta* **1968**, *162*, 327.

(15) Brühlmann, U.; Hayon, E. *J. Am. Chem. Soc.* **1974**, *96*, 6169.

(16) Kosower, E. M.; Teuerstein, A.; Burrows, H. D.; Swallow, A. J. *J. Am. Chem. Soc.* **1978**, *100*, 5185.

(17) Srividya, N.; Ramamurthy, P.; Shanmugasundaram, P.; Ramakrishnan, V. T. *J. Org. Chem.* **1996**, *61*, 5083.

(18) The symbol for this compound matches the nomenclature of refs 2 and 3.

(19) Timpe, H.-J.; Ulrich, S.; Fouassier, J.-P. *J. Photochem. Photobiol. A* **1993**, *73*, 139.

(20) Srividya, N.; Ramamurthy, P.; Ramakrishnan, V. T. *Spectrochim. Acta A* **1998**, *54*, 245.

(21) Karolczak, S.; Hodyr, K.; Łubis, R.; Kroh, J. *J. Radioanal. Nucl. Chem.* **1986**, *101*, 177.

(22) Gębicki, J.; Marcinek, A.; Rogowski, J. *Radiat. Phys. Chem.* **1992**, *39*, 41.

(23) Gritsan, N. P.; Zhai, H. B.; Yuzawa, T.; Karweik, D.; Brooke, J.; Platz, M. S. *J. Phys. Chem. A* **1997**, *101*, 2833.

(24) Becke, A. D. *J. Chem. Phys.* **1993**, *98*, 5648.

(25) Lee, C.; Yang, W.; Parr, R. G. *Phys. Rev. B* **1988**, *37*, 785.

(26) Frisch, M. J.; Trucks, G. W.; Schlegel, H. B.; Gill, P. M. W.; Johnson, B. G.; Robb, M. A.; Cheeseman, J. R.; Keith, T.; Petersson, G. A.; Montgomery, J. A.; Raghavachari, K.; Al-Laham, M. A.; Zakrzewski, V. G.; Ortiz, J. V.; Foresman, J. B.; Cioslowski, J.; Stefanov, B. B.; Nanayakkara, A.; Challacombe, M.; Peng, C. Y.; Ayala, P. Y.; Chen, W.; Wong, M. W.; Andres, J. L.; Replogle, E. S.; Gomperts, R.; Martin, R. L.; Fox, D. J.; Binkley, J. S.; Defrees, D. J.; Baker, J.; Stewart, J. P.; Head-Gordon, M.; Gonzalez, C.; Pople, J. A. *Gaussian 94*, revisions B1 and D4; Gaussian, Inc.: Pittsburgh, PA, 1995.

(27) For a description of the DFT methods implemented in the Gaussian program, see the following. Johnson, B. G.; Gill, P. M. W.; Pople, J. A. *J. Chem. Phys.* **1993**, *98*, 5612.

(28) Stratmann, R. E.; Scuseria, G. E.; Frisch, M. J. *J. Chem. Phys.* **1998**, *109*, 8218.

(29) Frisch, M. J.; Trucks, G. W.; Schlegel, H. B.; Scuseria, G. E.; Robb, M. A.; Cheeseman, J. R.; Zakrzewski, V. G.; Montgomery, J. A., Jr.; Stratmann, R. E.; Burant, J. C.; Dapprich, S.; Millam, J. M.; Daniels, A. D.; Kudin, K. N.; Strain, M. C.; Farkas, O.; Tomasi, J.; Barone, V.; Cossi, M.; Cammi, R.; Mennucci, B.; Pomelli, C.; Adamo, C.; Clifford, S.; Ochterski, J.; Petersson, G. A.; Ayala, P. Y.; Cui, Q.; Morokuma, K.; Malick, D. K.; Rabuck, A. D.; Raghavachari, K.; Foresman, J. B.; Cioslowski, J.; Ortiz, J. V.; Stefanov, B. B.; Liu, G.; Liashenko, A.; Piskorz, P.; Komaromi, I.; Gomperts, R.; Martin, R. L.; Fox, D. J.; Keith, T.; Al-Laham, M. A.; Peng, C. Y.; Nanayakkara, A.; Gonzalez, C.; Challacombe, M.; Gill, P. M. W.; Johnson, B. G.; Chen, W.; Wong, M. W.; Andres, J. L.; Head-Gordon, M.; Replogle, E. S.; Pople, J. A. *Gaussian 98*, revision A5; Gaussian, Inc.: Pittsburgh, PA, 1998.

(30) Bally, T.; Albrecht, B.; Matzinger, S.; Sastry, M. G.: *MOPLOT* (a program for displaying results of LCAO-MO calculations), version 3.2; University of Fribourg, Switzerland, 1997. Available from Thomas.Bally@unifr.ch on request.

(31) Haselbach, E.; Schmelzer, A. *Helv. Chim. Acta* **1979**, *54*, 1299.